Preparation Method and Physicomechanical Properties of EPS Lightweight Compaction-Filling Thermal Insulation Grouting Material

Letian Zhang[1], Huan He[1*], Dingwen Zhang[1], Songyu Liu[1,2]

[1]Southeast University, Jiangsu, Nanjing 210000, China
[2]Jiangsu Key Laboratory of Low Carbon and Sustainable Geotechnical Engineering, Jiangsu, Nanjing 210000, China

[*]Corresponding author: Huan He, e-mail: 360868337@qq.com

Abstract. Challenges are faced in the repair of local deformation diseases of roadbeds in permafrost regions. Grouting roadbed repair materials with both permafrost engineering adaptability and cost-effectiveness need to be developed urgently. EPS lightweight compaction-filling thermal insulation grouting material was proposed. Based on the three-factor and three-level orthogonal test and the method of controlled variables, physicomechanical indicators were measured. These indicators included negative temperature unconfined compressive strength, flowability, initial setting time, thermal conductivity, mass and strength loss rates of freeze-thaw cycles, and heat of hydration. The influence of each factor on the indexes was analyzed systematically. Material mix proportions suitable for filling and compaction grouting in permafrost engineering were optimized. Distribution images of aggregates and matrix were established by industrial CT. Results show that the optimal mix proportion of the material is as follows: the mass fraction of perlite is 50%, the water-cement ratio is 0.5, the content of polypropylene fiber is 0.1%, the content of fly ash is 20%, and the Superplasticizer dosage is 0.2%. A positive effect on aggregate anti-floating and anti-segregation is possessed by EPS modification and mix proportion design. The heat transfer mode of the grouting material tends to the series model, indicating that the skeleton conduction is effectively blocked by light aggregates, and ideal thermal insulation performance is obtained. Core parameters are provided by the research results for the mix proportion of EPS lightweight compaction-filling thermal insulation grouting materials. Broad application prospects are possessed in compaction and filling grouting engineering in permafrost regions.

Keywords: Roadbed repair; Grouting material; Thermal insulation; Negative temperature curing.

E. S. Zahran et al. (eds.), *Proceedings of the 2026 9th International Symposium on Traffic Transportation and Civil Architecture (ISTTCA 2026)*, Atlantis Highlights in Engineering 46,
https://doi.org/10.2991/978-94-6239-740-8_8

1 Introduction

Permafrost refers to rock or soil layers that remain at or below 0 °C for at least two consecutive years. Uneven frost heave and thaw settlement in permafrost lead to roadbed cracking and differential deformation, severely damaging transportation infrastructure in these regions. Additionally, global warming-induced permafrost thawing and active layer thickening are expected to worsen these effects[1, 2].

For the rehabilitation of existing road diseases, active cooling measures such as ventilation pipes and thermosyphons are commonly employed in projects including the Qinghai-Tibet Highway and Railway, effectively regulating permafrost temperature and mitigating associated infrastructure damage.[3, 4]. However, for localized deformation issues in existing roadbeds, passive reinforcement measures are still required for timely repair. Grouting in permafrost subgrades or foundations can achieve prompt rehabilitation and ground strengthening. Cement-based grouts are commonly used to repair permafrost-induced road damage due to their high compressive strength, wide availability, and relatively low cost, making them a cost-effective solution for infrastructure rehabilitation[5, 6]. However, conventional cement-based grouts have significant limitations, including high heat of hydration, high thermal conductivity, slow hardening and reduced strength under sub-zero curing, and poor resistance to freeze-thaw cycles. To address these limitations, modified cement-based grouts and novel chemical grouts have been developed. For example, partially replacing ordinary Portland cement with fly ash reduces the heat of hydration, while substituting with calcium sulfoaluminate cement accelerates hardening and enhances early-age strength.[7, 8]. In recent years, low-exothermic polymer grouting technology has also been introduced, characterized by low heat release, low thermal conductivity, high strength under sub-zero conditions[9]. However, existing cement-based grouts still have high thermal conductivity and poor freeze-thaw resistance, while novel chemical grouts are limited in widespread use due to their higher cost. Therefore, developing grouting materials for roadbed repair that balance both permafrost engineering requirements and economic feasibility remains a critical technical challenge.

EPS (Expandable Polystyrene) beads are closed-cell foam particles produced by physically foaming polystyrene resin with a blowing agent. Owing to their low density and excellent thermal insulation properties, they are often used in combination with other insulating materials such as perlite and glass microspheres. They can serve as lightweight aggregates in cement-based composites for building envelopes and subgrade insulation layers in permafrost regions[10, 11]. Studies have shown that hydrophilic modification of EPS with triethanolamine (TEA) or polyvinyl alcohol, followed by a “sand-coating” process, can effectively improve its dispersion in cement paste and enhance its affinity with the cement matrix[12]. Meanwhile, adding polypropylene fibers can effectively reduce shrinkage and cracking of EPS-cement composites at low temperatures.[13]. Furthermore, appropriate incorporation of expanded perlite into the EPS system can improve the composite strength[14]. Based on these characteristics, modified EPS beads can be used as lightweight fillers in cement-based grouts, with perlite added to optimize the particle-size gradation. In areas with loose soil or severe deformation after thawing and subsidence of permafrost, grouting materials can be used for compaction grouting to densify the surrounding soil, improving its strength and frost heave resistance, and enhancing thermal stability. When large voids occur due to frost heaving or thaw subsidence, filling grouting can be applied for repair. Additionally, with global warming accelerating permafrost degradation, pre-thawing technology can ensure long-term stability[15]. In such projects, modified EPS cement-based slurry fills the post-thaw voids, reinforcing weak soil layers and improving thermal stability due to its excellent insulation properties.

Based on above considerations, this study proposed a lightweight grouting material composed of ordinary Portland cement (OPC), calcium sulfoaluminate cement (SAC), fly ash, modified EPS beads, expanded perlite, and polypropylene fibers. Polycarboxylate ether (PCE) superplasticizer and anhydrous $CaCl_2$ are also incorporated to adjust workability and prevent freezing. The material performance was evaluated using the following indicators: unconfined compressive strength under negative temperature and pressure, flowability, initial setting time, heat of hydration, thermal conductivity, and mass and strength loss rates after freeze-thaw cycles. Through orthogonal preliminary tests, the effects of curing conditions, water-cement ratio (W/C), perlite content (by mass of lightweight aggregates), and fiber dosage (by mass of cementitious materials) on the performance indicators were analyzed. On this basis, influences of fly ash content (by mass of cementitious materials) and water-cement ratio on the material properties were investigated in subsequent experiments. This approach enables a systematic analysis of the material's physicomechanical properties under negative temperature and pressure, verifying its applicability and determining the optimal mix proportion.

2 Materials and Methods

2.1 Raw Materials

Modifier: Triethanolamine (analytical grade), produced by Sinopharm Chemical Reagent Co., Ltd., China. Portland cement: P·O 42.5 ordinary Portland cement, produced in Anhui, China. Calcium sulfoaluminate cement: R·SAC 42.5 rapid-hardening calcium sulfoaluminate cement, produced in Langfang, Hebei, China. Fly ash: Grade I fly ash, produced in Shenzhen, Guangdong, China. EPS beads: Expandable polystyrene foam particles, produced in Shenzhen, Guangdong, China, with a diameter of 0.5-1 mm. Perlite: Expanded perlite, produced in Xinyang, Henan, China, with a particle size of 1-4 mm and a bulk density of 95 kg/m^3. The basic physical properties of the two lightweight aggregates are listed in Table 3. $CaCl_2$: Anhydrous calcium chloride (analytical grade), produced by Sinopharm Chemical Reagent Co., Ltd., China. Superplasticizer: Polycarboxylate-based superplasticizer, produced in Shanghai, China. Fibers: Short polypropylene fibers, produced in Hebei, China, with a length of 6-8 mm. The main chemical compositions of the cement and fly ash are listed in Table 1 and Table 2, respectively. The key physical properties of the lightweight aggregates are provided in Table 3, wherein the bulk density of the lightweight aggregates was determined according to GB/T 17431.2-2010, and the thermal conductivity was measured by the transient hot-wire method.

Table 1. Main chemical compositions of OPC and SAC

Types of cement	SiO_2	Al_2O_3	CaO	Fe_2O_3	K_2O	MgO	Na_2O	SO_3
OPC	25.06	11.60	51.44	3.77	0.92	2.11	0.49	3.65
SAC	13.83	26.40	35.29	2.97	0.49	2.29	0.32	16.49

Table 2. Main chemical composition of fly ash

Composition	SiO_2	Al_2O_3	CaO	Free iron oxide	Cl^-	Iron content	Alkali content	Water content
Content (%)	45.1	36.8	4.5	0.85	0.015	0.85	0.75	0.40

Table 3. Main physical properties of lightweight aggregates

Type of aggregates	Bulk density (kg/m^3)	Thermal Conductivity (W/(m·K))
Modified EPS beads	110	0.0485
Expanded perlite	95	0.0560

2.2 Experimental Design and Parameter Settings

To achieve sufficient modification of EPS beads, this study employed a 20 wt% TEA solution for surface treatment, followed by a "sand-coating" process using a cement paste with a water-cement ratio of 1:1. To simulate the characteristic low-temperature and low-pressure environment of alpine permafrost regions (e.g., the Qinghai-Tibet Plateau), the specimens were cured at a sub-zero temperature of −3 °C, and a constant pressure of 50 kPa was maintained during both sample preparation and curing. To prevent freezing of the mixture, a 10% $CaCl_2$ solution was used as the mixing liquid, ensuring a freezing point below -3 °C. To balance thermal insulation, anti-flotation capability, and injectability, the wet density of the material was designed to be 1050 kg/m^3. To shorten the initial setting time and enhance increase compressive strength under sub-zero conditions, the mass ratio of OPC to SAC was set to 8:2[16]. Fly ash was incorporated at 10%, 20%, and 30% by mass of the cementitious materials. To identify a water-cement ratio that ensures both anti-segregation and adequate injectability, values of 0.4, 0.5, and 0.6 were selected. Perlite was added to the lightweight aggregates to optimize the particle-size distribution, with its content (by mass of lightweight aggregates) set at 0%, 25%, and 50%; the exact dosage was adjusted based on the target wet density. In addition, polycarboxylate superplasticizer (PCE) was added at 0.1%, 0.2%, and 0.3% by mass of cementitious materials, and polypropylene fiber at 0.1%, 0.15%, and 0.2% by mass of cementitious materials. To investigate the influence of different environmental parameters on the physicomechanical properties of the grouting material, three experimental groups were set up: normal temperature and normal pressure (NN), low temperature and normal pressure (LN), and low temperature and low pressure (LL).

To comprehensively investigate the influence of various factors on the physicomechanical properties of the grouting material, this study was conducted in two experimental phases. In the first phase, a three-factor, three-level orthogonal experimental design was applied to nine groups. The selected factors were perlite content (by mass of lightweight aggregates, denoted as A), fiber dosage (by mass of cementitious materials, denoted as B), and water-cement ratio (denoted as C). Their effects on the unconfined compressive strength (UCS), flowability, initial setting time, and thermal conductivity under sub-zero temperature and low-pressure conditions were examined. Based on the test results, analysis of range variance were performed. By comparing the range (R) and the significance of variance (p-value) at different levels, the optimal combination of the three factors was determined. The influence of curing conditions on the 28-day UCS and initial setting time of the grouting material was also analyzed. After determining the optimal reference mix proportion (denoted as T) from the orthogonal experiments, the controlled-variable method was further employed to systematically investigate the effects of fly ash content (denoted as D) and superplasticizer dosage (denoted as E) on the UCS, flowability, initial setting time, and thermal conductivity under sub-zero and low-pressure conditions, aiming to screen the final mix proportion with the best overall performance. Finally, the optimal mix proportion was tested for heat of hydration and freeze-thaw cycles to verify its hydration characteristics and frost resistance, providing a foundation for engineering applications. The detailed experimental plan is presented in Table 4.

The specimen preparation process is illustrated in Figure 1. Firstly, the required solid constituents were weighed and dry-mixed until homogeneous. Subsequently, a 10 wt% $CaCl_2$ solution was prepared and blended with the dry materials to form a slurry. The resulting slurry was stirred in a mixer for 120 s, then poured into molds. The molds were placed in the corresponding environmental conditions for curing. After 3-4 days of curing, the specimens were demolded and continued to be cured under the same conditions until the specified curing age was reached.

The modification of EPS beads was carried out according to the following procedure: a 20 wt% TEA solution was poured into an empty container; a predetermined amount of EPS beads was added to the container and mechanically stirred at 150 r/min for 1–3 min; the beads were then removed and air-dried at room temperature for 1 day. This process was repeated for three times. Subsequently, a cement paste with a water-cement ratio of 1:1 and a ratio of OPC-to-SAC of 8:2 was prepared and poured into an empty container. The treated EPS beads were placed in a container and stirred at 180 r/min for 2–5 minutes, then retrieved and air-dried for 1 day to obtain the modified EPS beads. The unconfined compression test was performed in accordance with JTG 3420-2020, using a compression testing machine. The flowability test followed GB/T 2419-2005, and a cement mortar flowability tester was employed. The initial setting time was determined according to GB/T 1346-2024 with a Vicat apparatus. The heat of hydration was measured in accordance with GB/T 12959-2024 using a TAM AIR isothermal calorimeter (USA). Thermal conductivity was tested in compliance with GB/T 10295-2008, employing a NETZSCH HFM 436/3/1E heat-flow-meter apparatus. The freeze-thaw cycle test was conducted following JTG 3420-2020. In compliance with JTG B01-2014, the uniaxial compressive strength loss after 25 freeze-thaw cycles was adopted as the evaluation indicator for the frost resistance of the grout. Industrial CT scanning was performed using a v|tome|x m 300 CT system with a resolution of 35 μm.

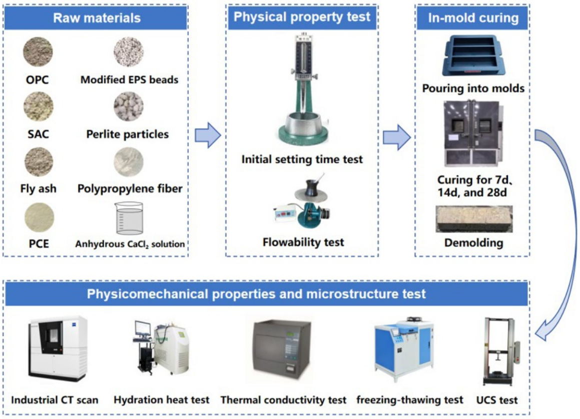

Fig. 1. Flow chart of specimen preparation

Table 4. Test program for physico-mechanical properties of grouting material

Group label	Curing condition	Perlite content (%)	Fiber content (%)	W/C	Fly ash content (%)	superplasticizer dosage (%)
$A_1B_1C_1$		0	0.1	0.4	0	0.2
$A_1B_2C_2$		0	0.15	0.5	0	0.2
$A_1B_3C_3$		0	0.2	0.6	0	0.2
$A_2B_3C_3$		25	0.2	0.6	0	0.2
$A_2B_1C_2$	LL, NN, LN	25	0.1	0.5	0	0.2
$A_2B_2C_1$		25	0.15	0.4	0	0.2
$A_3B_2C_1$		50	0.15	0.4	0	0.2
$A_3B_3C_2$		50	0.2	0.5	0	0.2
$A_3B_1C_3$		50	0.1	0.6	0	0.2
T-D_1E_1		50	0.1	0.5	10	0.1
T-D_1E_2		50	0.1	0.5	10	0.2
T-D_1E_3		50	0.1	0.5	10	0.3
T-D_2E_1		50	0.1	0.5	20	0.1
T-D_2E_2	LL	50	0.1	0.5	20	0.2
T-D_2E_3		50	0.1	0.5	20	0.3
T-D_3E_1		50	0.1	0.5	30	0.1
T-D_3E_2		50	0.1	0.5	30	0.2
T-D_3E_3		50	0.1	0.5	30	0.3

*For each test group, the specimens cured under LL conditions consisted of nine 40 mm × 40 mm × 160 mm parallel samples for compressive strength testing (three parallel samples per curing age) and two 300 mm × 300 mm × 15 mm parallel samples for thermal conductivity testing. The specimens cured under LN and NN conditions each comprised three 40 mm × 40 mm × 160 mm parallel samples for compressive strength testing (cured for 28 days).

3 Test Results and Discussion

3.1 Effect of Curing Conditions on the Physicomechanical Performance of Grouting Materials

The 28-day unconfined compressive strength (UCS) of specimens under different curing conditions is shown in Figure 2(a). A comparison of the results of NN and LN groups reveals that the UCS of the grouting material decreases significantly under sub-zero temperature and normal pressure. In the cementitious system, anhydrous calcium sulfoaluminate in sulfoaluminate cement reacts rapidly with gypsum and water to form ettringite and aluminous gel, creating an early framework. This reaction has a low apparent activation energy, making it fast and less temperature-sensitive, and is the main source of early strength. However, once calcium sulfoaluminate is depleted, the material strength primarily comes from the reaction of tricalcium silicate with water to form calcium silicate hydrate (C-S-H) gel, which has a higher apparent activation energy and is more temperature-sensitive. Since the system is dominated by Portland cement, the 28-day unconfined compressive strength of the grouting material significantly decreases[17]. A comparison between the LN and LL groups indicates that the UCS under sub-zero temperature and low pressure is slightly lower compared to that under sub-zero temperature and normal pressure. This can be attributed to the lower boiling point of water under reduced pressure, which promotes the evaporation of moisture both inside and on the surface of the cement paste. This leaves irregular pores within the paste, increasing the number of harmful pores and reducing the material's strength. However, in the grouting material system, EPS particles and perlite partially replace the pores in the cementitious material, thereby partially compensating for the strength loss[18]. Nevertheless, sub-zero temperature still remains the dominant factor affecting the UCS of the grouting material. Under LL curing conditions, the 28-day strength of all specimens exceeds 1.5 MPa, meeting the strength requirement for grouting materials in permafrost regions.

The initial setting time of specimens under different curing conditions is presented in Figure 2(b). Comparison of the NN and LN groups shows that the initial setting time of the grouting material increases significantly under sub-zero temperature, which is consistent with the reduction in UCS. The early hydration reaction of sulfoaluminate cement, which constitutes only 16% by mass of the cementitious system, cannot make the initial setting time at low temperatures equivalent to that at room temperature. It is worth noting that when the water-cement ratio increases to 0.6 (groups $A_1B_3C_3$, $A_2B_3C_3$, and $A_3B_1C_3$), the grout changes from a plastic to a fluid state, leading to a viscosity decrease. This reduction in viscosity delays the development of the hydration-product network, leading to a more pronounced extension of the initial setting time. Under sub-zero temperature, the hydration rate is low, and the accumulation of hydration products proceeds slowly. In fluid grouts, the hydrated product network forms more slowly, while in plastic-flow grouts, the high viscosity accelerates the early hydration network, speeding up initial setting. A comparison of the LN and LL groups indicates that, with respect to sub-zero temperature and normal pressure, the initial setting time under sub-zero temperature and low pressure generally exhibits a slight increase. Compared to normal pressure at low temperatures, under low pressure and low temperature conditions, although moisture evaporation decreases the effective water-to-cement ratio and increases ion concentration, the lower pressure raises the system's free energy, increases solution viscosity, and reduces ion mobility. This hinders nucleation of hydration products and slows down the cement hydration rate. For groups $A_1B_3C_3$, $A_2B_3C_3$, and $A_3B_1C_3$ with a water-cement ratio of 0.6, the grout is in a fluid state, and the hydration rate plays a more dominant role in the setting time. Consequently, the extension of the initial setting time is more marked in these cases.

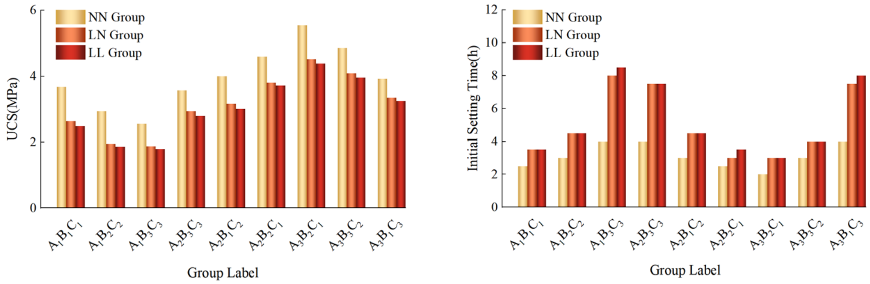

(a) (b)

Fig. 2. Test results of 28-day unconfined compressive strength for specimens under different curing conditions: (a) the UCS of each group; (b) The initial setting time of each group

3.2 Effects of Perlite Content, Fiber Addition, and Water-Cement Ratio on the Physicomechanical Performance of Grouts

Unconfined compressive strength under sub-zero temperature and low pressure. As shown in Figure 3, under sub-zero temperature and low-pressure conditions, the factors affecting the UCS are ranked in descending order of significance as follows: perlite mass fraction > water-cement ratio > fiber dosage. Among these, the perlite mass fraction and the water-cement ratio have a statistically significant effect on the UCS at different curing ages ($p < 0.05$), whereas the influence of fiber dosage is not statistically significant ($p > 0.05$). The perlite mass fraction exhibits the most pronounced impact. An increase in perlite content leads to a rise in UCS under sub-zero temperature and low pressure. Although the cylinder compressive strength of perlite and modified EPS beads is much lower than that of hydrated cement, perlite's elastic modulus is significantly higher than that of modified EPS beads. Hence, raising the perlite fraction enhances the overall stiffness of the composite, thereby improving its ability to transfer stress. Additionally, as expanded perlite particles have open pores, cement paste can penetrate the surface and shallow pores, creating a mechanical interlock and forming a strong interface. Additionally, the SiO_2 contained in perlite reacts with $Ca(OH)_2$ produced during cement, forming calcium silicate hydrate (C-S-H), which further contributes to strength development. The water-cement ratio ranks second. A decrease in water-cement ratio results in an increase in UCS under sub-zero temperature and low pressure. This is because a higher water-cement ratio results in more free water after hydration, and its subsequent evaporation creates pores in the hardened matrix, reducing compressive strength. Fiber dosage has the least effect on the UCS. Therefore, under sub-zero temperature and low-pressure conditions, appropriately increasing the perlite mass fraction and reducing the water-cement ratio can effectively enhance the UCS of the grouting material.

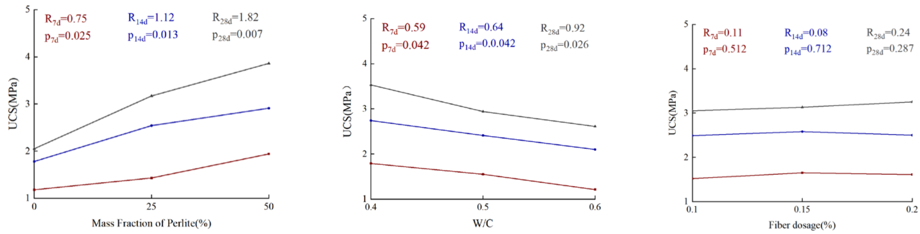

(a) (b) (c)

Fig. 3. Orthogonal test results of unconfined compressive strength under negative temperature and negative pressure: (a) affection of mass fraction of perlite; (b) affection of W/C ratio; (c) affection of fiber dosage

Flowability. As shown in Figure 4, the factors influencing the flowability of the grouting material are ranked in descending order of significance as follows: water-cement ratio > perlite mass fraction > fiber dosage. Among these, the perlite mass fraction and the water-cement ratio exhibit statistically significant effects on the flowability ($p < 0.05$), whereas the influence of fiber dosage on flowability is not statistically significant ($p > 0.05$). The water-cement ratio has the most pronounced impact on flowability. As the water-to-cement ratio increases, more free water is available for lubrication, reducing internal friction resistance. The increase in the water-to-cement ratio significantly lowers the system's viscosity, causing the system to transition from a plastic to a fluid state, which greatly enhances flowability. In the grouting material, as the water-cement ratio increases from 0.4 to 0.6, the material gradually shifts from a plastic-flow state to a fluid state. When the perlite mass fraction rises, the flowability shows a slight decrease. This is because perlite particles, being rough and porous compared to EPS beads, increase internal friction between particles in the paste, hindering the flow of the cement paste.

During compaction and filling grouting, if the flowability of the grouting material is too low, injection will be insufficient and construction will become difficult. Conversely, excessively high flowability indicates a transition from a plastic-flow to a fluid state, which promotes the flotation of lightweight aggregates and significantly weakens the compaction and reinforcement effects on the surrounding soil. According to GB 175-2023, the flowability of cement mortar should exceed 180 mm. At a water-cement ratio of 0.5, the flowability of the material is slightly above 180 mm, corresponding to a plastic-flow state. Therefore, a water-cement ratio of 0.5 provides the grouting material with both adequate injectability and effective compaction-reinforcement capability for the surrounding soil.

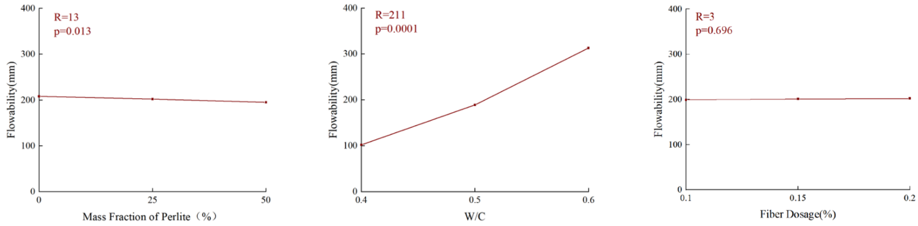

(a) (b) (c)

Fig. 4. Flowability test results of the orthogonal experiment: (a) affection of mass fraction of perlite; (b) affection of W/C ratio; (c) affection of fiber dosage

Initial Setting Time under sub-zero temperature and low pressure. As shown in Figure 5, under sub-zero temperature and low-pressure conditions, the factors influencing the initial setting time of the grouting material are ranked in descending order of significance as: water-cement ratio > perlite mass fraction > fiber dosage. Among these, the water-cement ratio exhibits a statistically significant effect on the initial setting time ($p < 0.05$), whereas the influences of fiber dosage and perlite mass fraction are not statistically significant ($p > 0.05$). When the water-cement ratio increases, the initial setting time under sub-zero temperature and low pressure is significantly prolonged. This is because, when the water-cement ratio increases, the concentration of cement particles per unit volume decreases, resulting in a lower ion concentration in the system, which slows down the hydration reaction rate. At the same time, the increased average distance between particles delays the interlocking process of hydration products, requiring more time to accumulate enough hydration products to form a continuous spatial network throughout the system. When the water-cement ratio increases to 0.6, the initial setting time extends more significantly compared to a ratio of 0.5, confirming the retarding effect of low viscosity on the initial setting time under sub-zero temperature and low pressure. Moreover, as the perlite mass fraction increases, the internal friction angle of the grouting material rises, increasing viscosity. This enhanced viscosity, combined with the incipient hydration-product network, resulting in a slight reduction in the initial setting time.

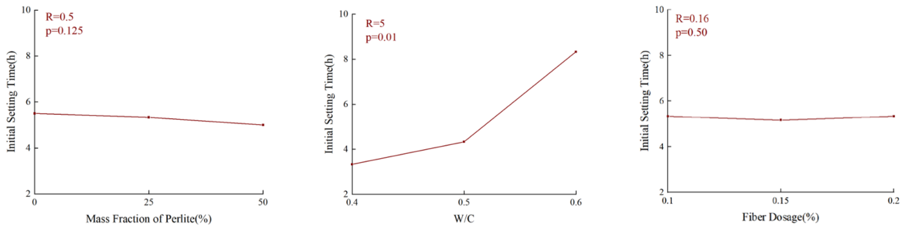

(a) (b) (c)

Fig. 5. Experimental results of initial setting time under negative temperature and negative pressure conditions: (a) affection of mass fraction of perlite; (b) affection of W/C ratio; (c) affection of fiber dosage

Thermal Conductivity. As shown in Figure 6, the factors influencing the thermal conductivity of the grouting material are ranked in descending order of significance as: water-cement ratio > perlite mass fraction > fiber dosage. Among these, the water-cement ratio has a statistically significant effect on thermal conductivity ($p < 0.05$), whereas the influences of perlite mass fraction and fiber dosage are not statistically significant ($p > 0.05$). As the water-cement ratio increases, the amount of mixing water rises correspondingly. The excess water gradually evaporates during the hardening of the cement, creating numerous pores within the material. These pores are filled with air, acting as an effective thermal insulator, enhancing the insulation capability of the material and reducing its thermal conductivity. However, the variation in thermal conductivity with the water-cement ratio is limited. Its magnitude remains primarily governed by the wet density of the material.

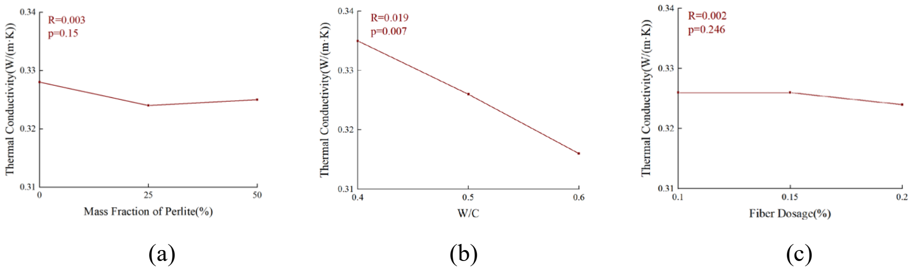

Fig. 6. Experimental results of thermal conductivity: (a) affection of mass fraction of perlite; (b) affection of W/C ratio; (c) affection of fiber dosage

3.3 Optimization of The Three Factors

To ensure the quality of grouting, the grouting material must possess adequate injectability and uniformity, high strength, low thermal conductivity, and a relatively short initial setting time. In this study, the performance indicators of the grouting material are prioritized in the following order: flowability > unconfined compressive strength (UCS) > thermal conductivity > initial setting time. Based on these criteria, the optimal combination of the three factors is determined as: a perlite mass fraction of 50%, a water-cement ratio of 0.5, and a polypropylene fiber dosage of 0.1%, i.e., group $A_3B_2C_1$. Thus, in the subsequent analysis, 'T' refers to group $A_3B_2C_1$.

3.4 Effects of Fly Ash and Superplasticizer on the Physicomechanical Performance of Grouts

The test results of the UCS of each group under sub-zero temperature and low pressure are shown in Figure 7(a). As can be seen, the UCS of the grouting material gradually decreases with increasing fly ash and superplasticizer contents. Fly ash is chemically inert in the early stages, almost not participating in chemical reactions. In the middle and later stages of hydration, as tricalcium silicate hydrates to form calcium hydroxide, the alkalinity of the system increases, triggering the pozzolanic reaction that requires a higher alkalinity. At this point, Al_2O_3 and SiO_2 in fly ash undergo pozzolanic reactions to form C-S-H products, which then interact with the hydration products from OPC and SAC to form a network. However, the pozzolanic reaction rate is highly temperature-dependent, and a decrease in temperature severely limits the reaction rate, while the lower temperature also slows down the formation of calcium hydroxide[19]. Thus, the 28-day curing period is insufficient for the full development of the cementitious contribution of fly ash. Meanwhile, under the same W/C ratio, a higher superplasticizer dosage results in more superplasticizer molecules adsorbing onto the surfaces of cementitious particles, which hinders the connection between the particles and water molecules. In addition, the polycarboxylate superplasticizer has some air-entraining properties, which increase the porosity of the system, resulting in a slight decrease in unconfined compressive strength. Nevertheless, although the addition of fly ash and superplasticizer reduces the UCS, the 28-day UCS of the grouted material under different curing environments remains at a relatively high level. This is due to the increased alkalinity, which accelerates the hydration reaction rate of fly ash, causing its hydration reaction rate at 28 days to remain higher than that in the early age period. When the fly ash content is less than 20 %, the 28-day UCS of the grouting material under sub-zero temperature and low pressure still maintains a relatively high value exceeding 3 MPa. Furthermore, it can be anticipated that the strength of the grouting material will further increase at longer curing ages such as 60 days and 90 days[20].

The flowability test results of the grouting material are presented in Figure 7(b). The figure indicates that increasing either the superplasticizer or fly ash content enhances the flowability. The superplasticizer can enhance the repulsive forces between cement particles, leading to a more uniform dispersion of the particles, which in turn releases water originally trapped within the cement particle agglomerates. In addition, As the mass fraction of the superplasticizer increases, the molecules adsorb onto the surface of the cementitious material particles, hindering the contact between water molecules and the cementitious materials, thereby releasing more free water that can be used for lubrication. Fly ash, as a fine material with smooth particles, reduces the frictional resistance between solid particles and exerts a lubricating effect. The influence of superplasticizer dosage on flowability is significantly greater than that of fly ash. As the superplasticizer dosage rises from 0.1 % to 0.3 %, the grouting material gradually shifts from a plastic-flow state toward a fluid state, approaching a fluid state at 0.3 %. When the superplasticizer content is 0.1 %, the flowability of the grouting material is too low, resulting in inadequate injectability. At a superplasticizer dosage of 0.3 %, the fluidity is excessively high. A superplasticizer content of 0.2 % provides the grouting material with a balanced combination of injectability, workability, and compaction-reinforcement capability for the surrounding soil.

The initial setting time test results of the grouting material are displayed in Figure 7(c). The figure shows that increasing of both fly ash and superplasticizer contents prolongs the initial setting time. This is because a higher superplasticizer dosage increases the adsorption of its molecules on cementitious particles, which retards the hydration reaction, and a greater fly ash content slows the early-age hydration rate. It is noteworthy that when the superplasticizer dosage reaches 0.3 %, the grouting material approaches a fluid state, leading to a substantial extension of the initial setting time under sub-zero temperature, similar to the mechanism by which the water-cement ratio affects the setting time.

The thermal conductivity test results of the grouting material are illustrated in Figure 7(d). Increasing the contents of both fly ash and superplasticizer reduces the thermal conductivity. This is because the later-age hydration products of fly ash can effectively fill larger pores originally present in the grouting material, transforming them into finer pores that are filled with air—an excellent thermal insulator. Meanwhile, a higher superplasticizer dosage increases the amount of free water. After evaporation, it leaves more air-filled pores, which also act as efficient thermal insulators. In addition, the air-entraining properties of polycarboxylate superplasticizers can also lead to an increase in the porosity of the system. However, the variation in thermal conductivity with fly ash and superplasticizer contents is limited. Its magnitude remains primarily governed by the wet density of the material.

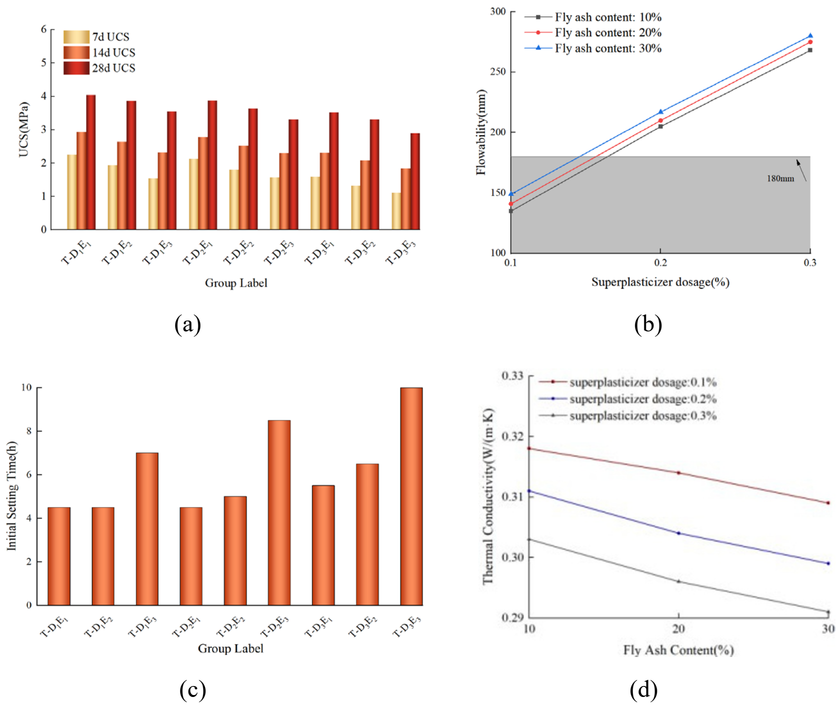

Fig. 7. Physicomechanical indicators test results of each group under negative temperature and negative pressure: (a) UCS; (b) flowability; (c) initial setting time; (d) thermal conductivity

3.5 Optimization of Mix Proportion and Performance Verification of Grouting Material

Following the same prioritization used in the three-factor, three-level orthogonal experiment, the performance indicators of the grouting material were ranked in order of importance as: flowability > UCS > thermal conductivity > initial setting time. To achieve optimal fluidity, uniformity, strength, and soil-reinforcement capacity simultaneously, the optimal fly ash content was selected as 20 % and the optimal superplasticizer dosage as 0.2 %. Accordingly, the final optimized mix proportion of the grouting material is: a perlite mass fraction of 50 %, a water-cement ratio of 0.5, a fiber dosage of 0.1 %, a fly ash content of 20 %, and a superplasticizer dosage of 0.2 %.

The variation of strength loss rate and mass loss rate of the grouting material with the number of freeze-thaw cycles is shown in Figure 8(a) and (b). As the number of freeze-thaw cycles increases, the rate of strength loss gradually slows down. This is because the repeated ice-expansion pressure induces micro-cracks inside the material, which provide buffer space for further ice-crystal growth. After 25 freeze-thaw cycles, the strength loss rate of the grouting material is only 8.37 %, and the residual strength still exceeds 3 MPa. The mass loss rate increases with the number of cycles, but the increment first rises and then declines. In the early stages of freeze-thaw cycling, the micro-cracks become pathways for water ingress. The absorbed water increases the mass of the specimen, partially offsetting the mass loss caused by surface scaling. During the first 5 cycles, the increase in mass loss rate is only 0.11 %. Between 5 and 10 cycles, the mass loss rate rises from 0.11 % to 0.87 %, after which the rate of increase slows. After 25 cycles, the mass loss rate reaches 1.94 %, which remains at a low level.

The cumulative heat of hydration versus time curves for the grouting material and a plain cement paste at 10 °C are presented in Figure 8(c). The plain cement paste had a binder proportion of OPC:SAC = 8:2, a water-cement ratio of 0.5, and contained no fly ash or lightweight aggregates. As seen in Figure 8(c), the incorporation of fly ash and lightweight aggregates significantly reduces both the total heat released and the rate of heat evolution. Compared with the EPS-modified grout, the plain cement paste exhibits a sharp, concentrated heat release at early ages, with a cumulative heat of 166.28 J/g within 63 h. In contrast, the hydration process of the EPS-modified grout is much gentler, releasing only 82.25 J/g over the same period. This demonstrates that the addition of fly ash and lightweight aggregates effectively reduces the heat of hydration, confirming the low-heat characteristic of the developed material.

In summary, the material satisfies the JTG 3420-2020 specification limits (strength loss after freeze-thaw cycles ≤ 25 %, mass loss ≤ 5 %) and possesses favorable hydration properties, indicating promising potential for application in permafrost subgrade rehabilitation.

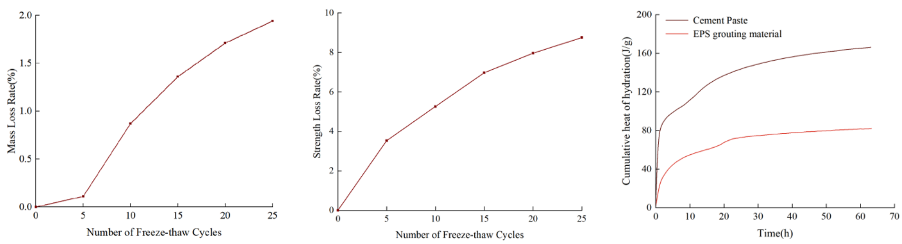

(a) (b) (c)

Fig. 8. Freeze-thaw durability and hydration performance indicators of grouting materials: (a) mass loss rate; (b) strength loss rate; (c) compressive rate of hydration

3.6 Microstructural Testing and Mechanism Analysis

A specimen with the optimized mix proportion and dimensions of 40 mm × 40 mm × 40 mm was prepared and scanned using industrial computed tomography (CT). To avoid edge artifacts, a central region of 35 mm × 35 mm × 35 mm was selected for three-dimensional reconstruction, as shown in Figure 9. The aggregate extraction plane was parallel to the yoz-plane, specifically the mid-plane of the specimen, located 20 mm from the edges. The measured porosity was 44.73 %. Figure 9 illustrates that the aggregates are uniformly distributed throughout the specimen, with no obvious flotation or segregation observed. This indicates that the optimized mix proportion effectively prevents aggregate buoyancy, validating the positive effect of EPS modification and mix design on reducing aggregate flotation and segregation.

The hardened grouting system primarily consists of a cementitious matrix, lightweight aggregates, and air pores. During heat transfer, thermal flow can either preferentially pass through the highly conductive cementitious matrix (parallel model) or sequentially move through each phase (series model), with the respective thermal conductivities calculated for each model.

At a wet density of 1050 kg/m^3, the total volume fraction of aggregates in the grouting material is calculated to be approximately 42.8 % based on the bulk densities of the two lightweight aggregates. In the industrial CT images, because the gray-scale values of aggregates and air pores are very similar, the measured porosity includes both aggregates and air pores. The calculated volume fraction of air pores in the grouting material is about 1.93 %. Additionally, a portion of sub-micron capillary pores could not be detected by industrial CT due to resolution limitations. Taking the thermal conductivity of the matrix as 1 W/(m·K), that of air as 0.026 W/(m·K), and that of the lightweight aggregates as 0.052 W/(m·K), the theoretical upper bound λ_{upper} (parallel model) and the theoretical lower bound λ_{lower} (series model) for the thermal conductivity of the grouting material can be calculated:

$$\lambda_{upper} = V_p \cdot \lambda_p + V_a \cdot \lambda_a + V_{air}\lambda_{air} = 0.575\text{W/（m}\cdot\text{K} \tag{1}$$

$$\lambda_{lower} = \frac{1}{\frac{V_p}{\lambda_p} + \frac{V_a}{\lambda_a} + \frac{V_{air}}{\lambda_{air}}} = 0.105\text{W/（m}\cdot\text{K} \tag{2}$$

Among these, V_p, V_a, V_{air} are relatively the volume fractions of the matrix, aggregates, and air pores in the total cementitious material; λ_p, λ_a, λ_{air} are relatively the thermal conductivity of the matrix, aggregates, and air pores in the total cementitious material. The measured thermal conductivity of the grouting material λ_e is 0.304W/(m· K), between the lower bound and the upperbound. Through the formula:

$$\lambda_e = d\lambda_{upper} + (1-d)\lambda_{lower} \tag{3}$$

The structural factor can be calculated as d=0.414, indicating that the heat-transfer mode of the grouting material lies between the two theoretical bounds and is closer to the series model. This suggests that the lightweight aggregates effectively interrupt the direct conductive pathways through the cementitious skeleton, thereby enhancing the material with desirable thermal insulation performance.

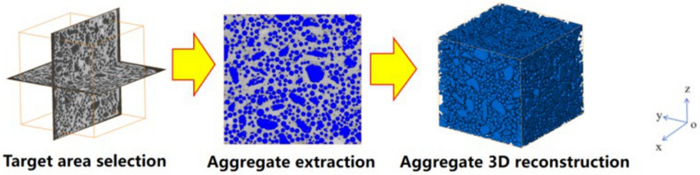

Fig. 9. Processed industrial CT images of grouting materials

4 Conclusion

To address the challenge of repairing roadbed distress caused by uneven frost heave and thaw settlement in permafrost, this study proposed an EPS lightweight compaction-filling and thermal insulation grouting material. A series of tests, including unconfined compressive strength under sub-zero temperature, flowability, initial setting time, thermal conductivity, freeze-thaw cycles, and heat of hydration, were conducted to investigate the physicomechanical properties of the EPS lightweight compacting-filling insulation grout. The experimental results demonstrate that:

(1) The final optimized mix proportion of the grouting material is as follows: a perlite mass fraction of 50 %, a water-cement ratio of 0.5, a fiber dosage of 0.1 %, a fly ash content of 20 %, and a superplasticizer dosage of 0.2 %. With this proportion, the grout exhibits balanced flowability, uniformity, strength, and soil-reinforcement capacity, showing significant potential for permafrost engineering applications.

(2) Under the optimized mix, after 25 freeze-thaw cycles, the grout shows a strength loss rate of 8.37 % and a mass loss rate of 1.94 %, both remaining at relatively low levels. The cumulative heat of hydration of the material at 10 °C is 82.25 J/g, confirming its excellent freeze-thaw resistance and low-heat characteristics.

(3) Industrial CT imaging shows a uniform distribution of aggregates within the sample, with no obvious flotation or stratification, confirming the effectiveness of EPS modification and mix design in preventing aggregate buoyancy and segregation. Heat-transfer analysis reveals that the grout's thermal conduction behavior falls between the series and parallel models, leaning more toward the series model. This confirms that the lightweight aggregates effectively interrupt the direct conductive pathways through the cementitious skeleton, providing the material with good thermal insulation performance.

Acknowledgments. The study was funded by National Key Research and Development Program of China (2023YFB2604800).

Disclosure of Interests. The authors have no competing interests to declare that are relevant to the content of this article.

Statement: DeepSeek was utilized to assist with primary translation and English language polishing of the manuscript.

References

1. SHAN, W.: Numerical Analysis of the Influence of Foundation Replacement Materials on the Hydrothermal Variation and Deformation Process of Highway Subgrades in Permafrost Regions. Water 14(17), 2642 (2022). https://doi.org/10.3390/w14172642.
2. WANG, Y.: Impact of Climate Change on the Performance of Permafrost Highway Subgrade Reinforced by Concrete Piles. Future Transportation 3(3), 996-1006 (2023). https://doi.org/10.3390/futuretransp3030055.
3. Du, S.: Analysis and Applications of the Two Phases Closed Thermosyphon Technology in the Highways in Permafrost Regions: A Review. Applied Sciences 14(10), 4185 (2024). https://doi.org/10.3390/app14104185.
4. Chen, X.: A preliminary study on the long-term structural stability of ventilation ducts in cold regions. Civil Engineering Journal 5(6), 1227-1234(2019). https://doi.org/10.28991/cej-2019-03091327.
5. Biggar, K. W.: Laboratory and field performance of high alumina cement-based grout for piling in permafrost. Canadian Journal of Civil Engineering 20(1), 100-106(1993). https://doi.org/10.1139/l93-011.
6. Reny, S., Pena, Cruz.: Development of a new cementitious grout for permafrost conditions. In J, Hadjigeorgiou., M, Hudyma. (eds) Proceedings of the Ninth International Symposium on Ground Support in Mining and Underground Construction 2016, pp. 533-544, Australian Centre for Geomechanics, Perth (2019). https://doi.org/10.36487/ACG_rep/1925_38_Reny.
7. LI, P.:Hydration mechanism and early frost resistance of calcium sulfoaluminate cement concrete. Construction and Building Materials, 239, 117862 (2020). https://doi.org/10.1016/j.conbuildmat.2019.117862.
8. Huo, J.: Thermal control effects and mechanism of slag and fly ash on heat development of cement slurry used in hydrate Formation. Journal of Natural Gas Science and Engineering, 91, 103967(2021). https://doi.org/10.1016/j.jngse.2021.103967.
9. ZHAO, L.: Properties of Low-Exothermic polymer grouting materials and its application on highway. Construction and Building Materials, 408, 133771(2023). https://doi.org/10.1016/j.conbuildmat.2023.133771.
10. LIN, J.: Development and Application of Graphene EPS Technology in Assembled Thermal Insulation Structural System: A Case Study of China's Severe Cold Regions. Advances in Civil Engineering, 2025(1), 4452245(2025). https://doi.org/10.1155/adce/4452245.
11. ZHANG, L.: A novel hydrophilic modification method of EPS particles: Conception design and performances in concrete. Cement and Concrete Composites, 142, 105199(2023). https://doi.org/10.1016/j.cemconcomp.2023.105199.
12. YUAN, J.: Study on frost resistance of EPS concrete based on EPS beads wrapping modification. Construction and Building Materials, 345, 128400(2022). https://doi.org/10.1016/j.conbuildmat.2022.128400.
13. Sadrmomtazi, A: An investigation on effect of using PP fibers and different cementitious materials on mechanical properties of EPS concrete. In: Proceeding of 3rd International Conference on Concrete & Development, pp. 1035-1044. Rilem, Qingdao. https://www.irbnet.de/daten/iconda/CIB13607.pdf.

14. Jadooe, A.: Effects of Silica Fume, Perlite, and Polypropylene Fibers on the Mechanical Properties of Lightweight Polystyrene Concrete Composite. Journal of Composites Science, 10(3), 124(2026). https://doi.org/10.3390/jcs10030124.
15. Cysewski, M. H.: Pre-Thawing: From Mining to Civil Engineering; A Historical Perspective. Cold Regions Engineering. 2009: Cold Regions Impacts on Research, Design, and Construction, 22-31(2009). https://doi.org/10.1061/41072(359)4.
16. Li, P.: Hydration mechanism and early frost resistance of calcium sulfoaluminate cement concrete. Construction and Building Materials, 239, 117862(2020). https://doi.org/10.1016/j.conbuildmat.2019.117862.
17. Trauchessec, R.: Hydration of ordinary Portland cement and calcium sulfoaluminate cement blends. Cement and Concrete Composites, 56, 106-114(2015). https://doi.org/10.1016/j.cemconcomp.2014.11.005.
18. Chen, X.: Influence of water-to-cement ratio and curing period on pore structure of cement mortar. Construction and Building Materials, 38, 804-812(2013). https://doi.org/10.1016/j.conbuildmat.2012.09.058.
19. Haha, M, B.: Quantification of the degree of reaction of fly ash. Cement and Concrete Research, 40(11), 1620-1629(2010). https://doi.org/10.1016/j.cemconres.2010.07.004.
20. Sivasundaram. V.: Long-term strength development of high-volume fly ash concrete. Cement and Concrete Composites, 12(4), 263-270(1990). https://doi.org/10.1016/0958-9465(90)90005-i.